

การสร้างรูปร่างคุณสมบัติของเปลวเพลิงเทอร์บิวเลนท์โดยวิธีแยกพิกเซลธรรมชาติ

Natural Pixel Decomposition Technique for Reconstructing

Turbulent-Flame Property Profiles

จีระวรรณ เกตุบุญ, ปุมยศ วลลิกุล, บัณฑิต ฟุ้งธรรมสาร
ศูนย์วิจัยการเผาไหม้ของเสีย ภาควิชาวิศวกรรมเครื่องกล คณะวิศวกรรมศาสตร์
สถาบันเทคโนโลยีพระจอมเกล้าพระนครเหนือ กรุงเทพฯ

Jeerawan Ketnuy, Pumyos Vallikul and Bundit Fungtammasan
The Waste Incineration Research Center (WIRC)
Department of Mechanical Engineering
King Mongkut's Institute of Technology North Bangkok

บทคัดย่อ

บทความกล่าวถึงการศึกษาขั้นตอนวิธีโทโมกราฟีแบบไม่ต่อเนื่องเพื่อสร้างภาพเสมือนของรูปร่างคุณสมบัติของเปลวเพลิงเทอร์บิวเลนท์ เปลวเพลิงที่ใช้ทดสอบในการสังเคราะห์ข้อมูลภาพถ่ายเป็นเปลวที่จำลองให้มีรูปร่างแบบทรงกระบอกสูงเอียงศูนย์ ซึ่งแทนสนามของการส่งผ่านเฉลี่ยแบบ 2 มิติ ได้นำวิธีการแยกพิกเซลธรรมชาติมาใช้ในขั้นตอนวิธีการสร้างภาพเสมือนเพื่อแก้ปัญหาที่มีตัวแปรมากกว่าสมการ โดยทำการศึกษาในรายละเอียดของเมตริกซ์พิกเซลธรรมชาติซึ่งแสดงคุณลักษณะของวิธีแยกพิกเซลธรรมชาติ รวมทั้งจำนวนมุมและจำนวนการเก็บข้อมูลแนวขวางที่เหมาะสมในการสร้างภาพเสมือน จากการศึกษาแสดงให้เห็นว่าวิธีการแยกพิกเซลธรรมชาติเป็นวิธีที่ทนทานต่อความไม่สมบูรณ์ของข้อมูลวิถีรวมในการสร้างภาพเสมือน และให้ผลที่สอดคล้องกับฟังก์ชันทดสอบ

Abstract

A discrete tomography reconstruction algorithm for reconstructing turbulent flame-property profiles has been studied. An artificial, off-centered "top-hat" profile representing a two-dimensional field of average value of transmittance of a turbulent flame is used as a test function. Limited projection data are generated from the test-function. The natural pixel (NP) decomposition technique for underdetermined problems has been used in this study with the matrix G , the characteristic matrix of the NP method, being examined in detail. The effects of the number of view angles and projection points on reconstruction results have also been investigated. It is found that the NP

technique tolerates incomplete data and yield good reconstruction results, which are in good agreement with the test function.

1. Introduction

Two-dimensional functions, $f(x,y)$, of moments of probability density functions for a particular region within turbulent flames can be represented by top-hat profiles [1,2,3,4]. An accurate reconstruction of the top-hat profiles from their tomographic data is a vital to the retrieval of thermodynamic probability density functions within turbulent flames[3,5]. Filter Back-projection (FBP) technique has been used successfully to reconstruct the moment functions for both symmetrical- and asymmetrical- turbulent flames [4]. The algorithm, however, needs excessive tomographic data in order to reconstruct accurately the moment functions.

Our previous work [6] suggested that reconstruction results from limited tomographic data can be obtained using either the Algebraic Reconstruction (ART) or Natural Pixel (NP) techniques. An off-centered gaussian profile was used as the test function. It also called for a more accurate numerical technique to treat matrix G , the characteristic matrix of the NP technique in order to obtain better reconstruction results.

In this paper, we review the definition of discrete tomography, NP technique and analyse G further and the pseudoinverse of the matrix G is calculated (see section 2). Reconstruction results of the off-centered tophat profiles are shown in section 3. At the end of section 3, a reconstruction from

incompleted data (view angles between 0-90°) is demonstrated through the NP and FBP techniques.

2. Descriptions

2.1 Discrete Tomography

In discrete tomography, the problem is derived in discrete form at the beginning of the reconstruction process. The two-dimensional domain is divided into $p \times p$ rectangular pixels and the function, $f(x,y)$, that falls into each pixel, is approximated to have a constant value f_q , ($q = 1 \dots p^2$), represented by a vector \underline{f} . The projection matrix ϕ , is then defined by the matrix that transforms the vector \underline{f} into the projection vector \underline{y} of length $M \times N$ where M and N represent the M view angles and the N number of projections at that view angle. Each element of \underline{y} then represents a strip projection of \underline{f} . The graphical concept of the discrete tomography is shown in figure 1.

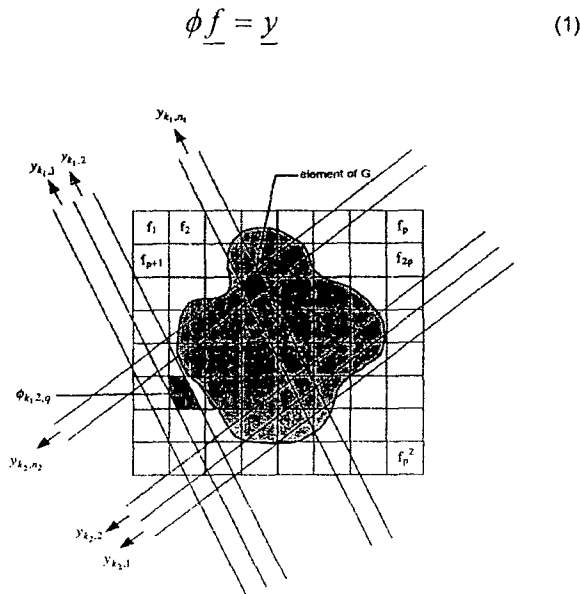


Figure 1 Determination of strip projection and projection matrix

2.2 Natural pixel decomposition and reconstruction

Natural pixel decomposition (NP) is a technique for reconstructing a square integrable function [7] from its incomplete tomographic data. With this technique, the vector \underline{f} is written as linear combinations of the column space of ϕ^T :

$$\underline{f} = \phi^T \underline{x} \quad (2)$$

where the elements of \underline{x} are unknown. The vector \underline{x} is

$$\underline{x} = [x^T(1) \quad x^T(2) \quad \dots \quad x^T(k) \quad \dots \quad x^T(M)]^T$$

and

$$x(k) = [x_{k1} \quad x_{k2} \quad \dots \quad x_{kn} \quad \dots \quad x_{kN}]^T$$

The vectors \underline{f} and \underline{x} and the matrix ϕ^T can be written in terms of their elements as

$$\begin{aligned} f_1 &= \phi_{1,1}x_{11} + \phi_{1,2}x_{12} + \dots + \phi_{1,n}x_{kn} + \dots + \phi_{1,N}x_{MN} \\ f_2 &= \phi_{2,1}x_{11} + \phi_{2,2}x_{12} + \dots + \phi_{2,n}x_{kn} + \dots + \phi_{2,N}x_{MN} \\ &\vdots \\ f_q &= \phi_{q,1}x_{11} + \phi_{q,2}x_{12} + \dots + \phi_{q,n}x_{kn} + \dots + \phi_{q,N}x_{MN} \\ &\vdots \\ f_{p^2} &= \phi_{p^2,1}x_{11} + \phi_{p^2,2}x_{12} + \dots + \phi_{p^2,n}x_{kn} + \dots + \phi_{p^2,N}x_{MN} \end{aligned} \quad (3)$$

Substitute \underline{f} from (2) into (1) and the result becomes

$$\begin{aligned} \underline{y} &= \phi \phi^T \underline{x} \\ \underline{y} &= G \underline{x} \quad \text{where} \quad G = \phi \phi^T \end{aligned} \quad (4)$$

G is the natural pixels matrix. As can be seen from (4) as well as figure 1, the element G_{ij} is a correlation between the i^{th} and the j^{th} strips. And the component y_i of the projection vector \underline{y} is the summation of all contribution of each correlation between the i^{th} and the j^{th} strips, starting from $j = 1$ to MN .

2.3 Evaluating the projection matrix: a simple example

Consider a domain consisting of 3×3 pixels and let each pixel have an area of unity. Two strips pass the pixels at the view angles of 0° and 90° respectively as shown in Figure 2.

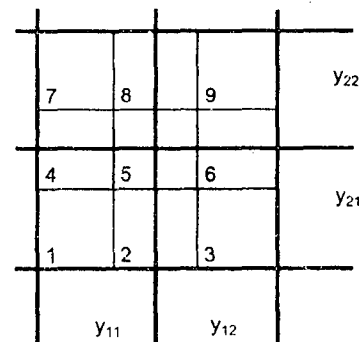


Figure 2 An example of function decomposition uses (3x3 pixels and 4 projection strips).

The matrix ϕ , according to (4), can simply be written as

$$\phi = \begin{bmatrix} 1 & 0.5 & 0 & 1 & 0.5 & 0 & 1 & 0.5 & 0 \\ 0 & 0.5 & 1 & 0 & 0.5 & 1 & 0 & 0.5 & 1 \\ 1 & 1 & 1 & 0.5 & 0.5 & 0.5 & 0 & 0 & 0 \\ 0 & 0 & 0 & 0.5 & 0.5 & 0.5 & 1 & 1 & 1 \end{bmatrix} \quad (5)$$

As can be seen from (5), ϕ_{11} is the intersection area of the strip y_{11} and pixel 1, ϕ_{12} is the intersection area of strip y_{11} and pixel 2, and so on.

2.4 Analysis of the matrix G

The characteristic matrix of NP method is studied here in detail. We are solving

$$G\underline{x} = \underline{y}$$

for \underline{x} . The problem yields a unique solution if and only if G is nonsingular. Determination of the determinants of all sizes of the matrix G used in this work indicates that it is nearly singular, so G has many solutions. Since rank(G) is less than its columns, least square solution is not unique. A partial replacement for the inverse is provided by the pseudoinverse.

The concept is to find B, a matrix of the same dimensions as G^T so that

$$\begin{aligned} G^* B^* G &= G \\ B^* G^* B &= B \end{aligned} \quad (6)$$

and GB and BG are Hermitian. The computation is based on singular value decomposition of G and any singular values less than a given tolerance are treated as zero.

The problem becomes

$$\underline{x} = B\underline{y} \quad (7)$$

which is the minimal norm solution, and also minimizes norm of \underline{x} .

3 Results

3.1 Test function and its projections

The top-hat profile has been chosen as the test function, $f(x,y)$ for this study. The function is of the form

$$f(x,y) = \begin{cases} \rho & \text{for } (x-x_0)^2 + (y-y_0)^2 \leq A^2 \\ 0 & \text{Otherwise} \end{cases} \quad (8)$$

where A, ρ , and (x_0, y_0) are set to be 0.35, 1, and (0.4, 0.0) respectively. A surface plot of the function is shown in Figure 3.

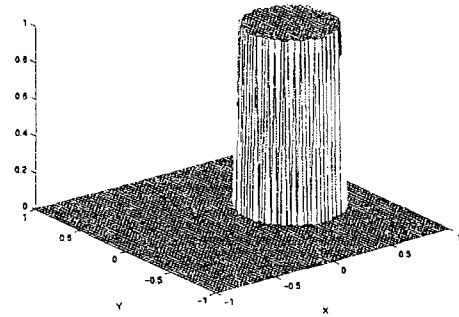


Figure 3 True function of Top-hat profile

The off-centered top hat profile has the analytical line integrated function at different angles of the form [8]

$$p_\theta(r) = \begin{cases} 2\rho\sqrt{(A^2 - r^2)} & \text{for } |r| < A \\ 0 & \text{for } |r| \geq A \end{cases} \quad (9)$$

The line integral (9) is used to calculate the analytical value of projection strips, that is

$$p_s(r_i) = \int_{r_i - \frac{\Delta}{2}}^{r_i + \frac{\Delta}{2}} p_\theta(r) dr = \begin{cases} \int_{r_i - \frac{\Delta}{2}}^{r_i + \frac{\Delta}{2}} 2\rho\sqrt{(A^2 - r^2)} dr, \text{ for } |r| < A \\ 0 & \text{for } |r| \geq A \end{cases} \quad (10)$$

Figure 4 and Figure 5 show the line and strip ($\Delta = 0.0317$) projections of the top hat profile at view angle 0° respectively. The line and the projection functions are respectively used in the FBP and the NP reconstruction algorithms. In line projection (Figure 4), at the rim point of the upper edge of the hat, even though the absorption coefficient is set to be 1, there is no path of attenuation; therefore, the projection at this point is zero.

In order to evaluate the resemblance between the test profile and its reconstruction results, we used the concept of "Picture distance" (PD) [9]: it is the normalized root-mean-square distance, d , as defined by

$$d = \sqrt{\frac{\sum_{i=k}^M \sum_{j=n}^N (T_{i,j} - R_{i,j})^2}{\sum_{i=k}^M \sum_{j=n}^N (T_{i,j} - T_{mean})^2}} \quad (11)$$

where T_{ij} is the value of original profile, R_{ij} is the reconstruction, and T_{mean} the average value of T_{ij} over the region of interest.

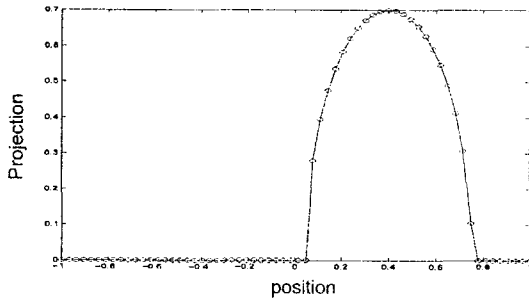


Figure 4 Projection of a top hat profile (64 sampling points)

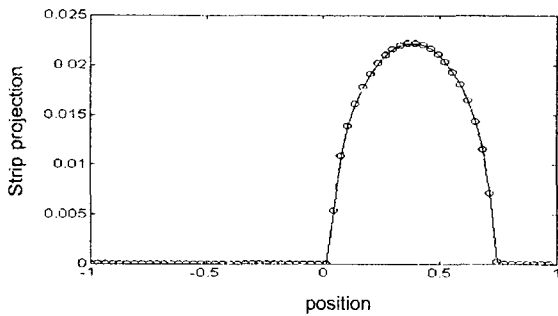


Figure 5 Strip projection of a top hat profile (64 sampling points)

3.2 Reconstruction from completed view angles

Effects of the number of angular samplings is studied at the appropriate number of pixels and number of lateral projections of 64x64 pixels and 64 points respectively.

It is shown in Figure 6 that most of the values of PD calculated from the FBP reconstruction results are higher than that from the NP reconstruction results. Figure 7 and 8 show the reconstruction results of NP and FBP techniques, respectively. It is clearly demonstrated that for a given number of the pixels and projections, a more accurate approximation function is obtained when more angular samplings are used. For FBP technique, noise like patterns [4,9] due to the under sampling of angular projections are notable. Conversely, NP technique tolerates the kind of error.

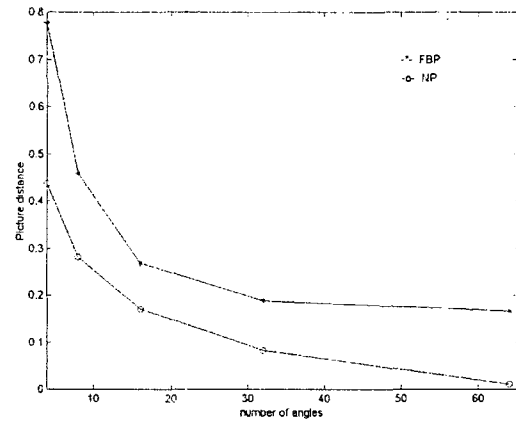


Figure 6 Picture distance : FBP and NP

3.3 Reconstruction from incompleting view angles

Reconstruction from incomplete data where only 90 degree projection are available (see Figure 9 and Figure 10) clearly demonstrated that the NP technique has the capability to reconstruct the test function from incomplete data. It is obvious that the FBP technique can only reconstruct a function from its complete projection data.

4. Conclusions

Discrete tomographic reconstruction of an off-centered top-hat function from its completed and incomplete data has been studied. With NP technique, its characteristic matrix, G , is analysed mathematically and found that it is close to singular. Pseudoinverse, then is introduced to solve this problem. Comparison the reconstruction results between two methods, FBP and NP, shows that NP gives more accurate reconstruction results than FBP, distinctively in the case of incomplete data. At the same time, it is found that the more view angles are used the more accurate reconstruction results can be obtained.

Acknowledgement

This work was supported in part by The Thailand Research Fund, Grant No. PDF/53/2540.

The computation parts of this work were performed using Matlab® software at the Faculty of Engineering Computing Facility, King Mongkut's Institute of Technology North Bangkok.

References

1. Sivathanu, Y.R. , and Gore, J.P. "A Tomographic Method for the Reconstruction of Local Probability Density Functions." *Journal of Quantitative Spectroscopy & Radiative Transfer* 50 (1993) : 483.

2. Nyden, M.R. ; Vallikul, P. ; and Sivathanu, Y.R.
 "Tomographic Reconstruction of The Moments of Local Probability Density Functions in Turbulent Flow Fields."
Journal of Quantitative Spectroscopy & Radiative Transfer
 55 No. 3 (1996) : 345-356.
3. Vallikul, P. ; Goulard, R. ; Mavriplis, C. ; and Nyden, M.R.
 "Tomographic Reconstruction of Probability Density Functions in Turbulent Flames." Conference Proceedings of The Seventh International Fire Science and Engineering Conference (Interflame'96), St. John's College, Cambridge, England, 26-28 March 1996 : 235-243
4. Meekunnasombat, P. ; Vallikul, P. ; and Fungtammasan, B.
 "A New Approach for Reconstructing Probability Density Functions in Turbulent Flames from Tomographic Data." Paper presented at The 12th National Mechanical Engineering Conference, Chulalongkorn University, Bangkok, 11-13 November 1998.
5. Vallikul, P. "Tomographic Reconstruction of Probability Density Function in Turbulent Flames." D.Sc. Thesis The School of Engineering and Applied Sciences , The George Washington University, 1996.
6. Meekunnasombat, P., Ketnuy, J., Vallikul, P., and Fungtammasan, B. Evaluation of An Algorithm for Discrete Tomographic Reconstruction of Turbulent Flame-property Profiles from Limited Data. The 13th National Mechanical Engineering Conference. Pattaya Chonburi 2-3 December 1999 : 291-296.
7. Buonocore, M.H. ; Brody, W.R. ; and Macovski, A. "A Natural Pixel Decomposition for Two-Dimensional Image Reconstruction." IEEE Transactions on Biomedical Engineering Vol. BME-28 No. 2 (February 1981) : 69-78.
8. Rosenfeld, A. , and Kak, A.C. Digital Picture Processing 2nd ed. New York : Academic Press, 1982.
9. Shigehito Suzuki "A Study on The Resemblance between A Computed Tomographic Image and The Original Object, and The Relationship to The Filter Function used in Image Reconstruction." Optik 66 No. 1 (1983) : 61-71.

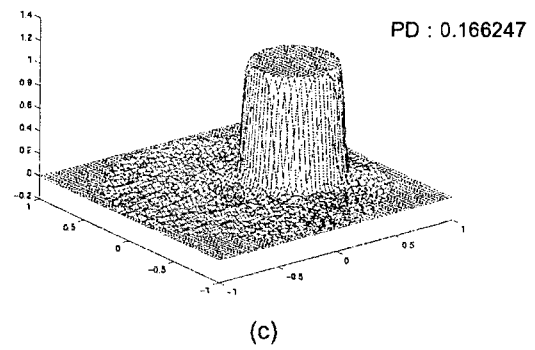
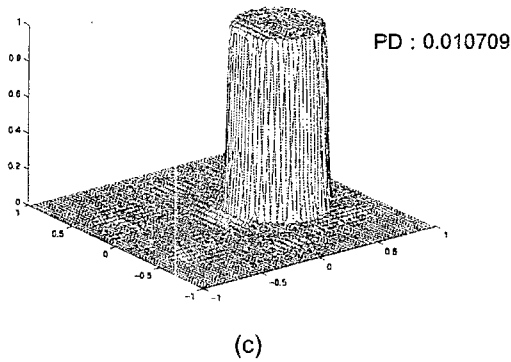
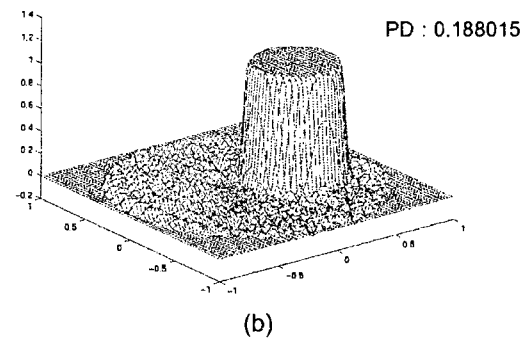
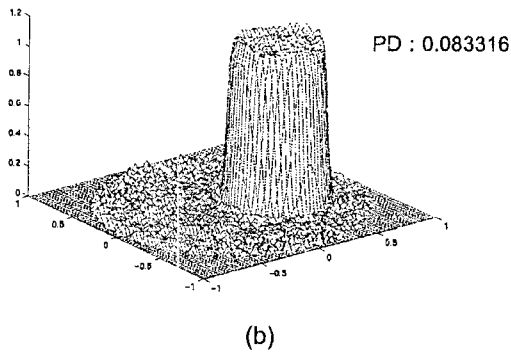
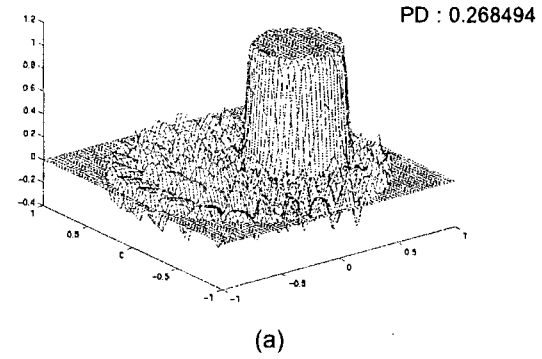
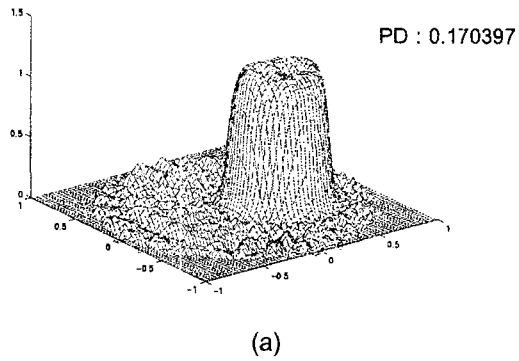


Figure 7 Reconstruction results using NP technique with 16, 32, 64 sampling angles respectively

Figure 8 Reconstruction results using FBP technique with 16, 32, 64 sampling angles respectively

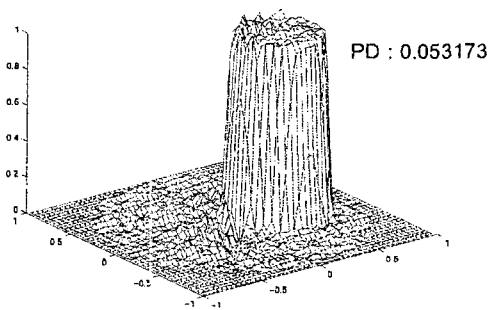


Figure 9 Reconstruction result from incomplete data using NP technique

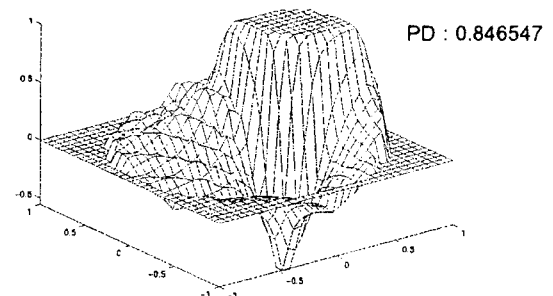


Figure 10 Reconstruction result from incomplete data using FBP technique